Dynamics of liquid silica as explained by properties of the potential energy landscape

A. Saksaengwijit and A. Heuer
Westfalische Wilhelms-Universitat Munster, Institut fur Physikalische Chemie Corrensstr. 30, 48149 Munster, Germany
(Dated: March 23, 2024)

The dynamics of silica displays an Arrhenius temperature dependence, classifying silica as a strong glass-former. Using recently developed concepts to analyse the potential energy landscape one can get a far-reaching understanding of the long-range transport of silica. It can be expressed in terms of properties of the thermodynamics as well as local relaxation processes, thereby extending the phenomenological standard picture of a strong glass-former. The local relaxation processes are characterized by complex correlated sequences of bond breaking and reformation processes.

PACS numbers: 64.70.Pf, 65.40.Gr, 66.20.+d

Silica is a prototypical and technologically relevant glass-former, displaying a variety of remarkable physical properties like thermodynamic anomalies [1, 2, 3]. In contrast to most other glass-formers the temperature dependence of its transport properties like the oxygen self-diffusion constant $D(T)$ display a simple Arrhenius behavior with an activation energy $V_{diffusion} = 4.7$ eV [4] and is thus a strong glass-former [5, 6]. This suggests that the transport can be described as a successive breaking and reformation processes of Si-O bonds with an activation energy close to $V_{diffusion}$ [7, 8].

To scrutinise this simple picture and thus to obtain a microscopic picture of the dynamics of silica we employ the framework of the potential energy landscape (PEL), defined in the high-dimensional configuration space [8]. At low temperatures the properties of silica and other glass forming systems are mainly characterized by the properties of the local potential energy minima of the PEL (denoted inherent structures, IS) [8, 9]. The thermodynamics of the system is mainly governed by the energy distribution of the number of IS. Introducing the configurational entropy $S_c(T)$ as a measure for the number of accessible IS at a given temperature, there is an empirical connection of $S_c(T)$ to the dynamics $D(T) \propto \exp(-A/TS_c(T))$ (Adam-Gibbs relation [10]) with some fitting parameter A [1, 11, 12]. Its theoretical foundation, however, is under debate [13, 14] and no direct interpretation of A is available, yet. In any event, one would expect that also the topology of the PEL should be of utmost importance for understanding the dynamics [15].

Following the ideas of Stillinger and Weber [9] one can map a trajectory, obtained via a molecular dynamics simulation, to a sequence of IS via frequent minimization of the potential energy. One example is shown in Fig. 1. This highlights how the system is exploring the PEL. One can group together IS to metabasins (MB) such that the dynamics between MB does not contain any correlated backward-forward processes [8, 16, 17]. Each MB is characterized by a waiting time τ and an energy e (defined as the lowest IS energy in this MB). The technical details of this approach, which have been developed in the context of studying a simple glass-forming model, i.e. the binary mixture Lennard-Jones system (BMLJ), can be found in [16].

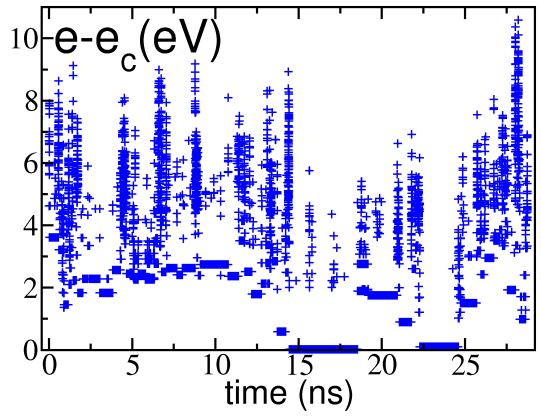

Figure 1: Time dependence of the IS energy e during a molecular dynamics simulation at $T = 3000$ K. The fountain-like objects correspond to time periods during which the system is moving very fast in configuration space. e_c is an estimate for the low-energy cutoff of the PEL.

In this work we apply these techniques to silica. Combining information about the energy distribution of IS and the local relaxation processes, reflecting the local topology of the PEL, we obtain a far-reaching understanding of its dynamics. From this we can identify the reasons why silica is a strong system and obtain a quantitative understanding of observables like the resulting activation energy $V_{diffusion}$. Further information is obtained from an appropriate comparison with the real-space behavior of silica. The underlying picture, emerging from these results, extends substantially the rationalization of the strong behavior of silica, sketched above.

Information about the BKS potential [18], used to model silica, as well as further simulation details can be found in Ref. [19]. For an optimum analysis in terms of the PEL the system size should be as small as possible without showing significant finite size effects [16]. It has been shown that already for system sizes $N \approx 10^2$ finite size effects concerning the configurational entropy [19], the properties of tunneling systems [20], the temperature dependence of the oxygen diffusion [19] as well as the nature of the relaxation processes in BKS silica (checked,

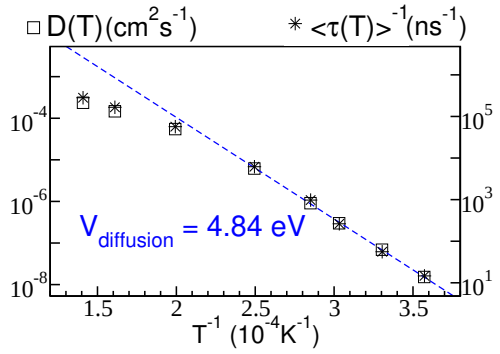

Figure 2: Temperature dependence of the oxygen diffusion constant $D(T)$ (macroscopic transport) and the inverse average waiting time $\langle (T)\rangle^{-1}$ (microscopic relaxation). The low-temperature activation energy is $V_{diffusion} = 4{:}84$ eV. Around 3500 K the so-called fragile-to-strong crossover is observed [1, 3, 12, 24].

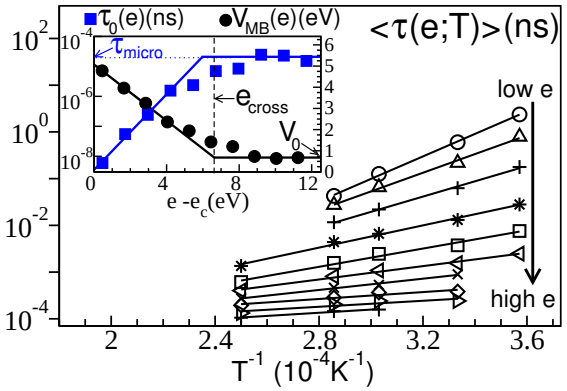

Figure 3: Arrhenius plot of the average MB waiting time $\langle (e;T)\rangle$ in dependence of energy (the chosen energy bins can be read off from the inset). $\langle (e;T)\rangle$ can be characterized by an effective activation energy $V_{MB}(e)$ and a prefactor $_0(e)$, shown in the inset. There exists a dynamic crossover energy e_{cross} such that for $e > e_{cross}$, $_0(e) = _{micro}$ 20 fs and $V_{MB}(e) = V_0$ 0:8 eV are roughly constant. The lines are guides to the eyes.

e.g., via the degree of non-exponentiality in the incoherent scattering function) [19, 21] are small in the accessible range of temperatures. Here we choose $N = 99$. Properties of larger systems can be then predicted from statistical arguments [22]. Recent studies have shown that the distribution of configurational energies has a low-energy cutoff around some energy e_c [19] with a finite configurational entropy [3]. It results from the network constraints in defect-free configurations [19]. It will turn out to be one key feature for the understanding of the dynamics.

In analogy to previous results for the BMLJ system [23] the oxygen diffusion constant $D(T)$ is proportional to the inverse of the average MB waiting time $\langle (T)\rangle$; see Fig.2. Thus, a local quantity like $\langle (T)\rangle$ fully determines the temperature dependence of diffusion, i.e. $d\ln D(T)=d$. The low-temperature activation energy $V_{diffusion} = 4{:}84$ eV is very close to the experimentally observed value of 4.7 eV [4]. Around 3500 K one observes the crossover from the high-temperature non-Arrhenius to the low-temperature Arrhenius-regime [1, 3, 12, 24].

One may suspect that the MB waiting times are strongly energy dependent because high-energy configurations have a larger number of defects [19] which can more easily relax [20]. For a quantification we determine the average MB waiting time in dependence of temperature and energy, denoted $\langle (e;T)\rangle$ from analysis of several independent equilibrium runs; see Fig.3. Interestingly, for all e one finds a simple Arrhenius-behavior, characterized by an effective activation energy $V_{MB}(e)$ and a prefactor $_0(e)$. Thus, the Arrhenius-behavior is not only present for simple atomic systems like the BMLJ system [16] but also for silica. One observes a crossover from the high-energy regime with $V_{MB}(e)$ V_0 and $_0(e) = _{micro}$ to a low-energy regime with a strong energy-dependence of both functions. The resulting broad distribution of waiting times implies that energy is likely the most dominating factor for understanding the occurrence of dynamic heterogeneities in silica and other glass-forming systems [25].

For relating the thermodynamics and the dynamics we introduce $p(e;T)$ as the Boltzmann probability to be in a MB of energy e. It turns out that in the relevant energy and temperature range $p(e;T)$ is virtually identical for MB and IS [19] and thus contains all the information about the configurational entropy. Using the quantities, introduced so far, we can write down the formal relation [16]

$$D(T) / \langle (T)\rangle^{-1} = \int dep(e;T)\langle (e;T)\rangle = \int dep(e;T)\frac{\exp(-V_{MB}(e))}{_0(e)}: \quad (1)$$

Its physical relevance is far-reaching because it relates the thermodynamics (via $p(e;T)$) and the local dynamics (via $\langle (e;T)\rangle$) to the long range diffusion. It follows that for very low temperatures for which $p(e;T)$ has only contributions for e e_c the dominant contributions to the average waiting time originate from configurations with energies close to e_c via $\langle (e$ $e_c;T)\rangle$. Then the local Arrhenius behavior $\langle (e$ $e_c;T)\rangle / \exp(-V_{MB}(e$ $e_c))$ translates into a macroscopic Arrhenius behavior. Indeed, the macroscopic activation energy $V_{diffusion}$ is close to $V_{MB}(e$ $e_c)$; see Fig.4.

What determines the value of the crossover temperature of 3500 K? At this temperature $p(e;T)$ is peaked around $e_c + 4$ eV and the low-energy wing of $p(e;T)$ just starts to be influenced by the low-energy cutoff [19]. Thus, on first view the above arguments to rationalize Arrhenius behavior should only apply for lower temperatures. However, due to the additional weighting of $\exp(-V_{MB}(e))$ by $1=_0(e)$ in Eq.1, which for e e_c is more than four orders of magnitude larger than $1=_{micro}$ ($_0(e$ $e_c)$ 5 10^3 fs), the influence of the low-energy

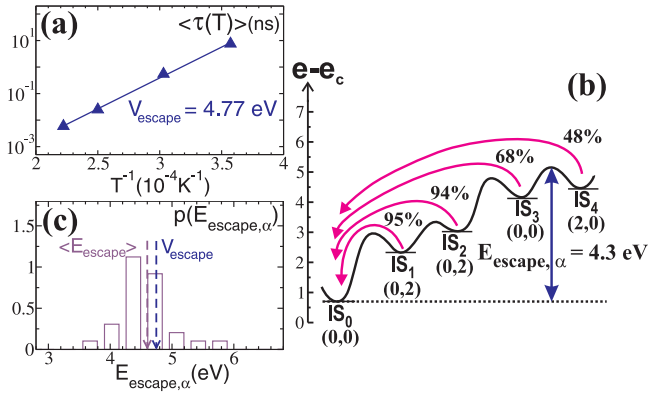

Figure 4: Detailed analysis of the escape properties from one defect-free low-energy structure IS_0. a) Temperature dependence of the average waiting time in IS_0. b) One specific escape path starting from IS_0. This representation reflects the sequence of inherent structure energies as well as saddle energies. The results for p_{back} are given above the arrows. The pairs of numbers at the bottom reflect the numbers of silicon and oxygen defects, respectively. The resulting effective barrier height $E_{escape;}$ is indicated. c) Distribution of $E_{escape;}$ and its average value $hE_{escape}i = 4:6$ eV (V_{escape}) for 30 different escape paths from IS_0.

states in the integral is significantly enhanced, thus giving rise to the actually observed crossover. Is there a direct relation to the mode-coupling temperature T_c 3300K [24]? Qualitatively, T_c is related to the beginning dominance of activated processes rather than to the presence of a low-energy cutoff of the PEL and thus seems to have a different physical origin.

In the next step we elucidate the microscopic origin of the escape properties from configurations close to e_c. We present detailed results for one specific configuration (denoted IS_0). In a first step we determine its average waiting time via repeated runs starting at IS_0 with different initial velocities and different temperatures. These runs typically involve many unsuccessful escape attempts. We define the waiting time as the time when IS_0 is left for the last time. We find a simple Arrhenius behavior with an effective activation energy of $V_{escape} = 4:77$ eV (Fig.4a).

This activation energy incorporates all the complexity of the local PEL around this configuration. In particular, the configuration may relax along different paths , which all contribute to the total relaxation rate, i.e. = . If p is the probability to escape via path and if path is characterized by an effective barrier height $E_{escape;}$ (see below for its definition) one can write $hE_{escape}i$ p $E_{escape;}$ [16], which is the average value of $E_{escape;}$ for independent runs starting from IS_0. A typical escape path is shown in Fig.4b. One can see the sequence of IS after IS_0 is visited for the last time. For every IS_i a value, denoted p_{back}, has been obtained from counting for a set of independent simulations with starting structure IS_i, whether or not the system returns to IS_0. Qualitatively, $p_{back} < 0:5$ indicates that the system will (on average) escape from the catchment region of IS_0. This limit typically involves the entropic effect that due to the large number of transition options in the high-dimensional PEL there is no need to follow the path back to IS_0. As shown in Ref.[16] for a given escape path a good estimate of $E_{escape;}$ is first to locate the first IS with $p_{back} < 0:5$ and then to identify $E_{escape;}$ as the highest energy along the reaction coordinate up to this IS. Application to the escape path in Fig.4b yields $E_{escape;} = 4:3$ eV. Four transitions are required until for the first time $p_{back} < 0:5$.

From the distribution of $E_{escape;}$ for 30 different escape paths from IS_0 one obtains $hE_{escape}i = 4:6$ eV which is close to the value of $V_{escape} = 4:77$ eV ; see Fig.4c. Thus, it is indeed possible to quantitatively relate the effective activation energy to the local properties of the PEL. Repeating this analysis for two different low-energy IS we get a similar agreement. More generally this implies that V_{MB} (e e_c), on the one hand, can be quantitatively related to specific local barriers and, on the other hand, to the activation energy of macroscopic diffusion $V_{diffusion}$. This establishes a direct link between the microscopic and macroscopic behavior of silica.

Having identified a complete escape process (relevant for $V_{diffusion}$) via the p_{back}-criterion we are in a position also to analyze its real-space characteristics. First we note that in the vast majority of cases the sequence of IS-transitions during the escape is correlated. This is reflected by the fact that at least one atom, involved in a bond-breaking or reformation process during a specific IS-transition (i 1) IS_i ! IS_{i+1} was involved during a previous IS-transition. When comparing IS_4 with IS_0 in total 4 Si-O bonds have been broken and 5 silicon atoms have changed their oxygen neighbors. These values are close to the average behavior after analyzing the escape from all three three initial IS (4.6 and 4.4, resp.). This implies significant correlated bond-breaking and reformation processes. In particular, $V_{diffusion}$ cannot be related to the breaking of a single Si-O bond. Other researchers have rationalized the value of $V_{diffusion}$ by the sum of half of the mean formation energy of an oxygen Frenkel pair and a migration barrier [21]. On a qualitative level something similar is observed here because in the first step a defect is created and afterwards the defect is transferred until $p_{back} < 0:5$. A closer look, however, reveals that the behavior in BKS silica is more complex as reflected, e.g., by the fact that in the example of Fig.4 in between also configurations with no defects occur (IS_3).

The additional contribution of the saddle between IS_3 and IS_4 of approx. 0.8 eV to the final value of $hE_{escape}i$ is small. This also holds in general (approx. 1.0 eV) which, interestingly, is close to V_0. Thus one may conclude that there are two distinct contributions to the activation energy V_{MB} (e): (1) V_{MB} (e) V_0 as the contribution reflecting the topology of the PEL, related to differences between IS energies, and (2) V_0 as the additional contribution of the final saddle. Around e e_c the first contribution is dominating.

Why is silica a strong glass-former? The standard scenario, sketched in the introductory paragraph, would imply $\langle e;T\rangle i \quad _{micro} \quad \exp(\ V_{diffusion})$ [7, 8]. This reflects the presence of one typical relaxation process which holds throughout the entire PEL [8]. In contrast, our simulations have revealed a strong energy dependence of $V_{MB}(e)$ and $_0(e)$ together with complex successive bond-breaking and reformation processes. Rather we can identify two underlying reasons for the classification of silica as a strong glass-former: (1) the presence of the cutoff in the PEL of silica as a consequence of its network structure, (2) the Arrhenius temperature dependence of $\langle e \quad e_c;T\rangle i$ together with a large attempt rate $1=_0(e_c)$. How to rationalize property (2)? As can be seen from Fig.4c the distribution of effective barrier heights $E_{escape;}$ is very narrow. For the example of IS_0 this implies an Arrhenius temperature dependence in agreement with the observation; see Fig.4a. This behavior was also observed for the escape from the other low-energy IS, analyzed along the same lines. Thus, it seems to be a general feature that starting from a low-energy (and typically defect-free) configuration around e_c the system first has to acquire an energy of approx. $e \quad e_c + V_{MB}(e_c)$ until the escape is complete (ending in an IS with $e \quad e_c + V_{MB}(e_c) \quad V_0$). More pictorially one may state that low-energy IS ($e \quad e_c$) form the bottom of crater-like objects in the PEL and the system has no escape option apart from climbing up the whole crater until $e \quad e_c + V_{MB}(e_c)$. Thus, beyond the presence of the low-energy bound of the PEL the strong behavior of silica is also related to this crater-like structure of the PEL.

The previous thermodynamic analysis has revealed that for this system the number of IS with $e_c + V_{MB}(e_c)$ $V_0 \quad e_c + 4$ eV is approx. 10^5 times larger than the corresponding number at $e \quad e_c$ [19]. This observation suggests that the number of possible transitions from $e \quad e_c$ to configurations with energies around $e_c + 4$ eV is also exponentially large, thereby rationalizing the dramatic increase of $1=_0(e_c)$ as compared to $1=_{micro}$. It has been already explicitly shown in previous model calculations that the prefactor for relaxation processes in model landscapes scales with the number of accessible states for which for the first time p_{back} is smaller than approx. 50% [26]. Then $1=_0(e_c)$ can be much larger than microscopic jump rates. Interestingly, in the relevant energy regime of the BMLJ system the number of IS increases much weaker with increasing energy and correspondingly there is hardly any energy-dependence of $_0(e)$ [16]. This further supports our hypothesis about the origin of the large energy-dependence of $_0(e)$.

It has been speculated that different network-forming systems (e.g. silica and water) have similar properties [27, 28, 29]. Indeed, indications have been found recently that also the amorphous states of water possesses a low-energy cutoff, which will influence the thermodynamics and dynamics at low temperatures similarly to silica [30]. Therefore exploration of the properties of silica may be of major importance also for an improved understanding of water and other network formers. The possible universality of this class of systems has recently lead to the formulation of an abstract model which is aimed to reflect the basic physics of all amorphous network formers [31].

In summary, using the PEL-framework we have identified relevant underlying mechanisms for the dynamics of silica: (1) The elementary relaxation processes are not simple bond-breaking processes with the final activation energy but rather form correlated sequences of many bond-breaking processes with a strong dependence on the initial energy. (2) The simultaneous presence of the low-energy cutoff of the PEL as well as the narrow distribution of escape barriers from MB give rise to the resulting strong behavior. (3) Dramatic entropic effects are present for the escape from low-energy states, showing that the dynamics is much more complex than reflected by the resulting simple Arrhenius behavior. (4) The occurrence of the crossover temperature around 3500 K can be quantitatively understood by the presence of the low-energy cutoff and these entropic effects. (5) There exists a crossover energy which separates the high-energy liquid-like behavior and the low-energy activated behavior.

We gratefully acknowledge helpful discussions with R. D. Banhatti, B. Doliwa, D. R. Reichman, O. Rubner and M. Vogel. The work was supported in part by the DFG via SFB 458 and by the NRW Graduate School of Chemistry.

[1] I. Saika-Voivod, P. H. Poole, and F. Sciortino, Nature 412, 514 (2001).
[2] M. S. Shell, P. G. Debenedetti, and A. Z. Panagiotopoulos, Phys. Rev. E. 66, 011202 (2002).
[3] I. Saika-Voivod, F. Sciortino, and P. H. Poole, Phys. Rev. E. 69, 041503 (2004).
[4] J. C. Mikkelsen, Appl. Phys. Lett. 45, 1187 (1984).
[5] C. A. Angell, Science 267, 1924 (1995).
[6] G. Ruocco et. al, J. Chem. Phys. 120, 10666 (2004).
[7] M. D. Ediger, Ann. Rev. of Phys. Chem. 51, 99 (2000).
[8] P. G. Debenedetti and F. H. Stillinger, Nature 410, 259 (2001).
[9] F. H. Stillinger and T. A. Weber, Phys. Rev. A 25, 978 (1982).
[10] G. Adam and J. H. Gibbs, J. Chem. Phys. 43, 139 (1965).
[11] S. Sastry, Nature 409, 164 (2001).
[12] E. La Nave, H. E. Stanley, and F. Sciortino, Phys. Rev. Lett 88, 035501 (2002).
[13] X. Xia and P. G. Wolynes, Phys. Rev. Lett 86, 5526 (2001).
[14] L. Berthier and J. P. Garrahan, Phys. Rev. E. 68, 041201

(2003).
[15] F. H. Stillinger and P. G. Debenedetti, J. Chem. Phys. 116, 3353 (2002).
[16] B. Doliwa and A. Heuer, Phys. Rev. E. 67, 031506 (2003).
[17] R. A. Denny, D. R. Reichman, and J. P. Bouchaud, Phys. Rev. Lett. 90, 025503 (2003).
[18] B. W. H. Van Beest, G. J. Kramer, and R. A. Van Santen, Phys. Rev. Lett. 64, 1955 (1990).
[19] A. Saksaengwijit, J. Reinisch, and A. Heuer, Phys. Rev. Lett. 93, 235701 (2004).
[20] J. Reinisch and A. Heuer, Phys. Rev. Lett 95, 155502 (2005).
[21] L. Martin-Samos, Y. Limoge, J. P. Crocombette, G. Roma, and N. Richard, Phys. Rev. B 71, 014116 (2005).
[22] D. J. Wales and J. P. K. Doye, J. Chem. Phys. 119, 12409 (2003).
[23] B. Doliwa and A. Heuer, Phys. Rev. E. 67, 030501 (2003).
[24] J. Horbach and W. Kob, Phys. Rev. B. 60, 3169 (1999).
[25] M. Vogel and S. C. Glotzer, Phys. Rev. Lett. 92, 255901 (2004).
[26] A. Saksaengwijit, B. Doliwa, and A. Heuer, J. Phys.: Condens. Matter 15, S1237 (2003).
[27] K. Ito, C. T. Moynihan, and C. A. Angell, Nature 398, 492 (1999).
[28] A. Scala, F. W. Starr, E. L. Nave, F. Sciortino, and H. E. Stanley, Nature 406, 166 (2000).
[29] H. E. Stanley et. al, J. Stat. Phys. 110, 1039 (2003).
[30] P. H. Poole, I. Saika-Voivod, and F. Sciortino, J. Phys. Cond. Matter 17, L431 (2005).
[31] A. J. Moreno et. al, Phys. Rev. Lett. 95, 157802 (2005).